I J Radiol. 2024 July; 21(3): e149360 https://doi.org/10.5812/iranjradiol-149360

Published Online: 2024 July 31

Research Article

Effectiveness of Twin-Beam Dual-Energy Computed Tomography in Characterization of Solitary Pulmonary Nodules Larger Than 5 mm

Saim Turkoglu [1,*], Mesut Özgökçe [2]

[1] Department of Radiology, Medical Faculty, Yuzuncu Yıl University, Van, Turkey
[2] Yuzuncu Yıl University, Van, Turkey

[*] ***Corresponding Author:*** Department of Radiology, Medical Faculty, Yuzuncu Yıl University, Van, Turkey. Email: mdsaimturkoglu@gmail.com

Received: 19 February, 2024; **Revised:** 19 July, 2024; **Accepted:** 23 July, 2024

Abstract

Background: Advancements in technology have significantly improved the diagnosis of solitary pulmonary nodules in the lungs. Various computed tomography (CT) imaging techniques, including modern dual-energy computed tomography (DECT), have enhanced the ability to accurately classify pulmonary nodules as benign or malignant. In this study, three different dual-energy parameters — iodine load, contrast load, and visual assessment — were evaluated for their potential in characterizing pulmonary nodules.

Objectives: The aim of this study was to assess the reliability and effectiveness of DECT in distinguishing benign from malignant pulmonary nodules using different parameters, including visual assessment, iodine concentration, and contrast load.

Patients and Methods: This prospective study included patients who underwent contrast-enhanced thoracic DECT for solitary pulmonary nodules, had histopathological examination results, or had at least a two-year follow-up CT scan. Patients with nodules smaller than 6 mm or completely calcified nodules were excluded. Patients diagnosed with a suspicious solitary pulmonary nodule on chest radiography and subsequently underwent contrast-enhanced DECT, or those diagnosed with a lung nodule on routine non-contrast CT scans and later evaluated using DECT, were included in the study. Benign and malignant nodules were compared based on gender, age, contrast load, iodine load, and color map assessment. Nodule images were obtained 40 seconds after intravenous contrast administration using single-source DECT (120 kV split filter) with twin-beam technology. The visual enhancement and color map evaluation, including contrast and iodine load measurements, were separately calculated and recorded for each lung nodule.

Results: A total of 59 patients [30 males (50.8%) and 29 females (49.2%)] with a solitary pulmonary nodule met the inclusion criteria. Among the 59 pulmonary nodules, 16 (27.1%) were malignant, and 43 (72.9%) were benign. Of the benign lesions, 23 (53.5%) were found in males and 20 (46.5%) in females. The mean age of patients with benign nodules was 53.5 ± 12 years (range: 25 - 73 years), while for those with malignant nodules, it was 69.2 ± 5.59 years (range: 57 - 75 years). There was no statistically significant difference in age between the two groups ($P = 0.506$). The median contrast load was 0.0 Hounsfield units (HU) [interquartile range (IQR: 64)] in benign nodules and 63 HU (IQR: 154) in malignant nodules. Malignant nodules had a significantly higher contrast load than benign nodules ($P = 0.003$). Using a cut-off value of 22 HU for contrast load in malignancy diagnosis, the sensitivity was 100%, specificity was 58.14%, positive predictive value (PPV) was 47.06%, and negative predictive value (NPV) was 100%. The area under the curve (AUC) was 0.746. The median iodine load was 0.0 mg/dL (IQR: 4.5) in benign nodules and 4.5 mg/dL (IQR: 11.8) in malignant nodules. Malignant nodules had a significantly higher iodine load than benign nodules ($P < 0.001$). Using a cut-off value of 1 mg/mL for malignancy diagnosis, the sensitivity was 100%, specificity was 62.79%, PPV was 50%, and NPV was 100% (AUC: 0.768).

Conclusion: Dual-energy computed tomography provides valuable contributions in differentiating benign and malignant pulmonary nodules. In this study, the diagnostic value of three different approaches — visual iodine coverage color map, iodine concentration, and contrast load — was demonstrated in distinguishing these lesions.

Keywords: Dual Energy, Benign, Malignant, Pulmonary Nodule, Twin-Beam, Iodine Map, Contrast Load, Iodine Load

1. Background

The use of imaging for diagnosing solitary pulmonary nodules has become increasingly widespread in recent years with advancements in various technological methods. Nowadays, dual-energy computed tomography (DECT) has made the characterization of pulmonary nodules easier and more reliable. This study aims to further explore these factors. A study by Gould et al. reported an increase in the lung nodule detection rate from 3.9 to 6.6 per 1,000 person-years and an increase in the lung nodule identification rate from 24 to 31 per 100 chest computed tomography (CT) scans between 2006 and 2012 (1). In this context, the characterization and early diagnosis of lung nodules are crucial, as they significantly impact survival and morbidity.

Solitary pulmonary nodules are commonly encountered during routine radiological evaluation of the thorax and may represent early manifestations of lung malignancies. However, distinguishing between benign and malignant nodules is often challenging due to the low sensitivity of both 18-fluorodeoxyglucose (FDG) positron emission tomography (PET) and CT-guided biopsy, particularly for smaller nodules (< 5 mm) (2). The limited accessibility, high cost, and time-consuming nature of PET-CT, along with the invasive nature and procedural risks of CT-guided biopsy, have driven the search for less invasive diagnostic methods.

Nodules larger than 5 mm should be followed up based on defined risk factors and specific nodule characteristics. Lung nodules that remain stable for at least two years are generally considered benign (3). Therefore, characterizing parenchymal nodules and differentiating between benign and malignant tumors is essential for early diagnosis and timely treatment.

Recent technological advancements have introduced DECT as a novel imaging technique that aids in differentiating benign from malignant lesions by assessing contrast enhancement. This imaging method allows for the evaluation of nodules based on their shape, size, margins, and internal composition. Additionally, DECT provides further assessment through contrast load, iodine load, and contrast enhancement imaging using dual-source techniques (4). While many studies have examined DECT findings in various pulmonary and vascular conditions, such as pulmonary thromboembolism and pulmonary hypertension, data on its use in distinguishing malignant from benign pulmonary nodules remain limited. Because DECT offers additional parameters, including visual assessment, iodine load, and contrast load, it is emerging as a superior alternative to conventional CT for pulmonary nodule evaluation.

2. Objectives

This study aims to evaluate the efficacy and reliability of DECT in distinguishing benign from malignant pulmonary nodules by comparing visual assessment, iodine load, and contrast load parameters in clinical use.

Today, DECT can be performed using either two X-ray tubes or a single X-ray tube operating at different tube currents. This technique allows for "dual-energy" scanning, enabling data acquisition at 80 kVp and 140 kVp (5). A greater difference between the tube currents (e.g., between 80 kVp and 140 kVp) enhances the differentiation of substances with varying densities (5). This technical advantage of DECT provides several benefits, including reduced radiation exposure compared to dynamic imaging studies and improved detection of calcifications (6).

A twin-beam DECT technique utilizes a split filter composed of tin and gold, positioned in front of the X-ray tube. This filter divides the 120 kVp X-ray beam into low- and high-energy spectra, which are then detected by a single detector (7).

In conventional dynamic CT scans, data are obtained by subtracting a baseline non-contrast image from contrast-enhanced images. Unlike conventional dynamic CT, DECT simultaneously acquires both non-contrast and iodine contrast-enhanced images in a single scan (8). As a result, DECT reduces radiation exposure and expands its clinical applications. This imaging modality appears useful for diagnosing pulmonary nodules without the need for a preliminary non-contrast scan.

3. Methods

3.1. Patient Selection

This study is a prospective, cross-sectional study and was approved by a university ethics committee under approval number 08 on May 15, 2018. The study was conducted at Van Yuzuncu Yil University Hospital in the Eastern Anatolia region, a medical center serving a population of approximately 4 million, specializing in advanced examination and treatment of lung diseases. Informed consent was obtained from all patients before participation. Patients were informed that DECT imaging is a contrast-enhanced examination with

potential complications similar to those of conventional CT. The standard consent procedure used in conventional CT examinations was also explained to them. Patient data were collected in Excel format and were accessible only to the principal investigator and sub-investigator to ensure data confidentiality. Patients referred to the radiology clinic due to suspected lung nodules or masses were included in this study. The inclusion assessment was conducted without prior knowledge of the underlying etiological factors. Patients who had undergone at least one contrast-enhanced thoracic DECT scan for a solitary pulmonary nodule and had either histopathological examination results (from a transthoracic, transbronchial, or excisional biopsy) or a minimum of two years of follow-up CT scans at a tertiary university hospital between 2017 and 2019 were included. The Dutch-Belgian Randomized Lung Cancer Screening Trial (NELSON study) determined that the risk of lung cancer development within two years is very low if the nodules remain unchanged during that period (3). The exclusion criteria were as follows: Patients with nodules smaller than 6 mm or completely calcified nodules were excluded. Completely calcified nodules were not included as they are most likely benign and could lead to falsely high iodine level and contrast load calculations. Patients without at least two years of follow-up CT scans or histopathological examination results were excluded. Patients with known systemic diseases and lung nodules that could have resulted from these conditions were excluded. Based on histopathological examination results or changes in size observed during follow-up CT scans, nodules were classified as either benign or malignant. Only solid solitary nodules were included in the study. Nodules associated with systemic disease or unknown metastases were excluded. A total of 59 patients with solitary pulmonary nodules were included. The study evaluated the relationship between benign and malignant nodules concerning gender, age, contrast load, iodine load, and color map findings.

3.2. Scanning Protocol

Dual-energy computed tomography scanning was performed using a specialized dual-energy protocol. All thoracic scans were obtained using the split-filter dual-energy mode (Siemens SOMATOM Definition AS+128, Forchheim, Germany). Tomographic examinations were conducted with a 512 × 512 pixel matrix, 64 × 0.6 mm collimation, a split filter (120AuSn) positioned in front of a 120 kV x-ray beam, 270 milliamperes (mA), and the dual-energy twin-beam mode of the SOMATOM Definition scanner (Siemens Medical Solutions) at a 0.7 pitch and 0.5-second rotation time. All scans were performed with the patient in the supine position in a craniocaudal direction, covering the entire thorax. An intravenous iodine contrast agent, iohexol (GE Healthcare's Omnipaque 350 mg/50 mL), was administered at a dose of 1.3 - 1.5 mL/kg at a rate of 1.6 mL/s using an automatic injector. Simultaneous scanning was performed with a split filter and 120 kV tube voltage (120AuSn) to obtain images. The 120 kV split-filter (120AuSn) dataset and the weighted average image dataset were transferred to a workstation (SyngoVia; Siemens Medical Solutions). The weighted average image, which could be used for routine 120 kV clinical applications, was automatically generated by combining the 140-kV and 80-kV data. Virtual non-contrast (VNC) and iodinated contrast-enhanced images were acquired on the workstation using a modified prototype of the Syngo Dual Energy (Siemens Medical Solutions), which functioned as a VNC application mode. Images were reconstructed on an axial dataset with a 3 mm slice thickness.

3.3. Image Analysis

Each nodule was evaluated by a radiologist with 14 years of experience in thoracic imaging who was blinded to the histopathological results and previous radiologic features of the patients. To minimize bias in image analysis, a second radiologist was consulted in cases of disagreement, and if necessary, a third experienced radiologist provided the final decision. The first evaluation involved a qualitative visual assessment, in which a VNC image of the iodine component in translucent mode was displayed as a background color overlay. The manufacturer-defined iodine retention value was set at higher than 50% for default color-coding. The presence of any color (orange or red) in the nodule was considered indicative of contrast enhancement, while a black color (no color-coding) was interpreted as the absence of contrast enhancement. The results were recorded in a binary format as "present" (orange-red) or "absent" (black) (Figures 1 and 2).

At least three regions of interest (ROIs) were manually drawn, depending on the lesion's diameter. The average value from multiple measurements within an ROI, placed as homogeneously as possible near the central part of each nodule, was recorded. Extreme outliers were excluded from the study. The mean of these measurements was then calculated. Using computer software, this average ROI measurement provided data on iodine presence and changes in HU

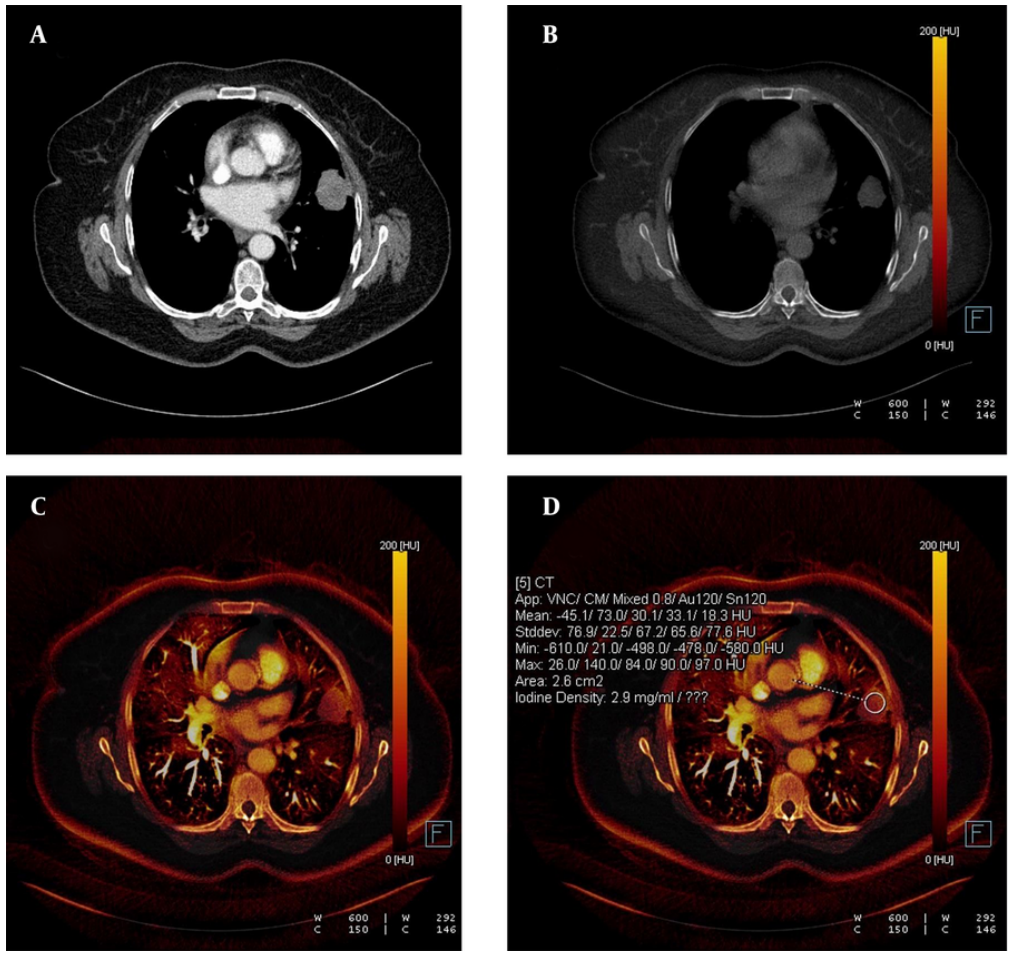

Figure 1. A, The weighted average image; B, The virtual non-enhanced image; C, The iodine-enhanced image; and D, The image of the iodine load are observed in dual-energy computed tomography, DECT. C - D, The iodine component is shown as a color overlay on a background virtual non-enhanced image in translucent mode.

values within the nodule. The second parameter analyzed was the attenuation change in density, expressed in HU, and the third parameter was iodine concentration, expressed in mg/mL (Figures 3 -7).

3.4. Statistical Analysis

The variables were presented as mean ± standard deviation. A Mann-Whitney U test was used to compare iodine and contrast loads between benign and malignant nodules. A receiver operating characteristic (ROC) analysis was performed to determine the cut-off value of iodine and contrast loads for differentiating malignant from benign lesions. A chi-square test was used to compare the color distributions (orange-red/black) of benign and malignant lesions. A P-value of < 0.05 was considered statistically significant. Statistical analyses were conducted using SPSS for Windows, version 21.0 (IBM Corp. Released 2012. IBM SPSS Statistics for Windows, Version 21.0. Armonk, NY: IBM Corp.).

4. Results

A total of 59 patients, 30 males (50.8%) and 29 females (49.2%), with a solitary pulmonary nodule met the inclusion criteria. Among the 59 pulmonary nodules, 16 (27.1%) were malignant, while 43 (72.9%) were benign. Of the benign lesions, 23 (53.5%) were detected in males and 20 (46.5%) in females. Among the 16 malignant lesions, 7 (43.8%) were observed in males and 9 (56.2%) in females. There was no statistically significant difference between male and female patients in terms of whether their lung

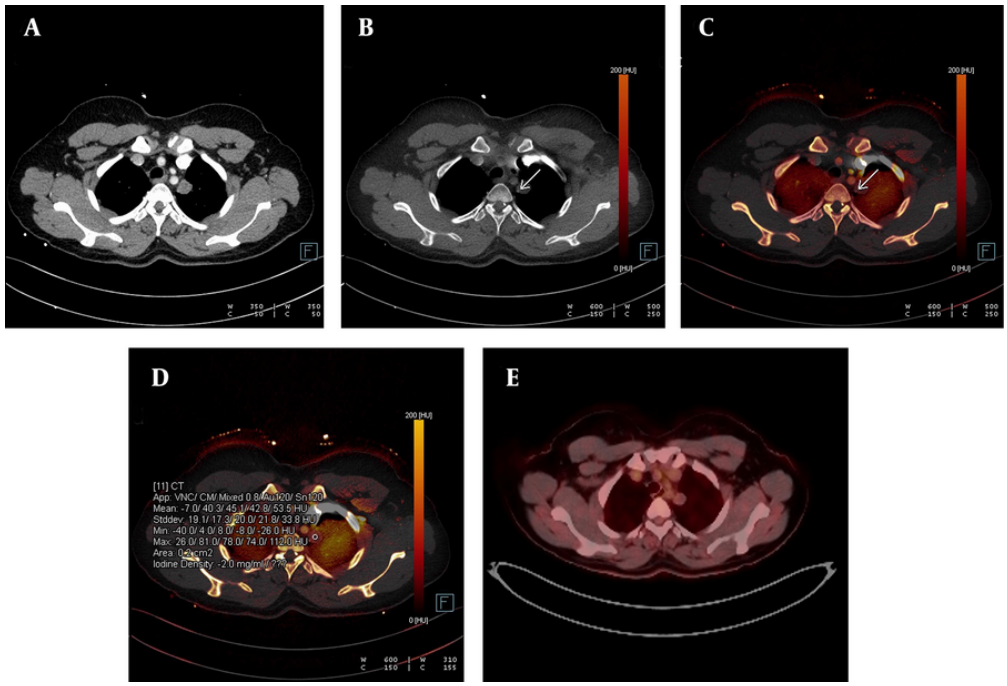

Figure 2. Detection of calcification in a lung nodule on a virtual non-contrast-enhanced image in dual-energy computed tomography, DECT. A, The weighted average image of the lesion in the apical segment of the left lung; B, The virtual non-contrast-enhanced image showing a small calcification around the nodule (white arrow); C, Dual view; and D, Iodine load are shown; E, No significant 18-FDG uptake was observed in the PET-CT images obtained from the same patient.

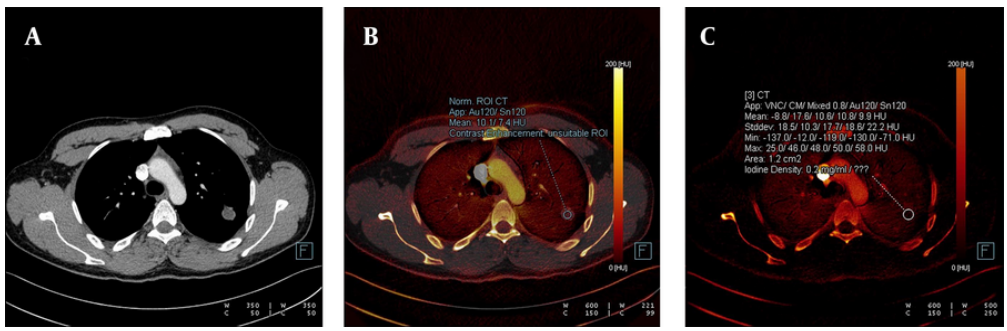

Figure 3. A, The weighted average image; B, The virtual iodine-enhanced dual image; and C, The image of the iodine load are shown in dual-energy computed tomography, DECT. A solitary pulmonary nodule with an infinitesimal contrast load and an iodine load of 0.2 mg/dL was observed. The diagnosis was confirmed as a hydatid cyst through histopathological examination.

nodules were benign or malignant (P = 0.506). The mean age of patients with benign nodules was 53.5 ± 12 years (age range: 25 - 73 years), while for those with malignant nodules, it was 69.2 ± 5.59 years (age range: 57 - 75 years) (P < 0.001). There was no statistically significant difference in age between the two groups (P = 0.506). The largest nodule had a maximum diameter of 30 mm, while the smallest measured 5 mm (Table 1).

The median contrast load was 0.0 Hounsfield units (HU) [interquartile range (IQR): 64] in benign nodules and 63 HU (IQR: 154) in malignant nodules. The contrast load of malignant nodules was significantly higher than

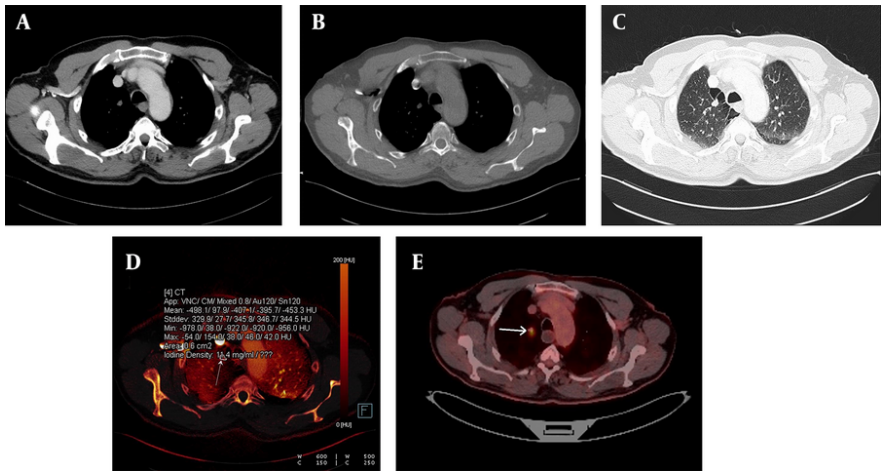

Figure 4. A malignant nodule is shown on an iodine-enhanced image. A, Weighted average image; B - C, Virtual non-enhanced images; and D, Iodine load in dual-energy computed tomography, DECT. In the iodine-enhanced image D, the iodine value was measured at 11.4 mg/dL. E, The malignant characteristics of the nodule were clinically confirmed and further validated via a PET-CT examination (white arrow). The PET-CT image corresponds to the same patient whose DECT images are presented above.

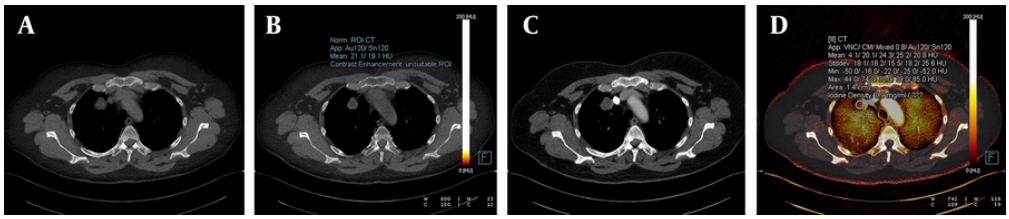

Figure 5. A benign lung nodule is shown on an iodinated image. The weighted average axial image (A), an image with no contrast load (B), the virtual iodine-enhanced image (C), and the iodine load (D) are shown in dual-energy computed tomography (DECT). Solitary pulmonary nodule with no contrast load (B) diagnosed as a benign hamartoma.

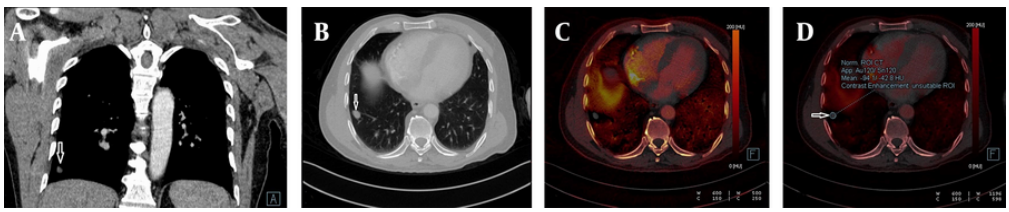

Figure 6. A benign lung nodule is shown on an iodinated image. The weighted average coronal (A), axial (B), virtual enhanced iodinated image (C), and the iodine load (D) are shown in dual-energy computed tomography (DECT). A benign solitary pulmonary nodule, where the contrast load is infinitesimal (white arrow). The solitary pulmonary nodule remained stable in the two-year follow-up period.

that of benign nodules (P = 0.003). Considering a cut-off point of 22 HU for contrast load in the diagnosis of malignancy, the sensitivity was 100%, specificity was 58.14%, positive predictive value (PPV) was 47.06%, and negative predictive value (NPV) was 100%. The area under the curve (AUC) was 0.746.

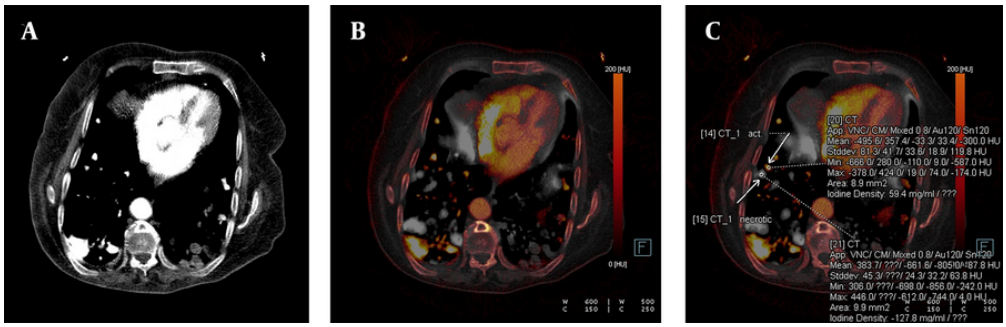

Figure 7. Confirmed metastatic lung nodules originating from colon cancer are shown on the iodine-enhanced image of the patient presenting with shortness of breath. The weighted average image (A), the virtual iodine-enhanced image (B), and the image of the iodine load (C) are shown in dual-energy computed tomography (DECT). On a weighted average image, it is difficult to determine whether the metastatic nodule responds to chemotherapy or not. However, it is easier to identify active and necrotic nodules by inspection on iodinated dual images (white arrows). The detection of the iodine load as 59.4 mg/mL in the active nodule and as negative values in the necrotic nodule are the supporting findings.

Table 1. Demographic Characteristics of Patients [a]

Variables	Total (n = 59)	Male (n = 30)	Female (n = 29)	P-value
Total patients	59	30 (50.8)	29 (49.1)	-
Malignant lesions	16 (27.1)	7 (11.8)	9 (15.2)	0.506
Benign lesions	43 (72.8)	23 (38.9)	20 (33.8)	
Mean Age of patients with benign nodules	53.5 ± 12 (25 - 73)	-	-	< 0.001
Mean age of patients with malignant nodules	69.2 ± 5.59 (57 - 75)	-	-	

[a] Values are expressed as No. (%) or mean ± SD (range).

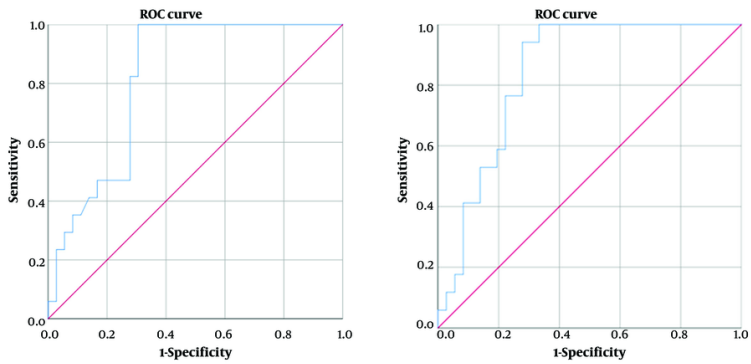

Figure 8. Receiver operating characteristic (ROC) curves calculated for iodine and contrast load are shown in the graphs, respectively.

The median iodine load was 0.0 mg/dL (IQR: 4.5) in benign nodules and 4.5 mg/dL (IQR: 11.8) in malignant nodules. The iodine load of malignant nodules was significantly higher than that of benign nodules (P < 0.001). Considering a cut-off value of 1 mg/mL for the diagnosis of malignancy, the sensitivity was 100%, specificity was 62.79%, PPV was 50%, and NPV was 100% (AUC: 0.768) (Figure 8).

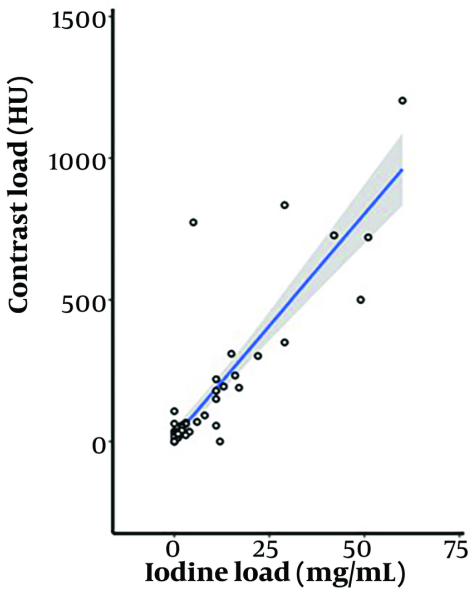

Figure 9. Correlation between contrast load and ion load

A strong correlation was observed between contrast load and iodine load, with a Spearman correlation coefficient of 0.862 ($P < 0.001$) (Figure 9).

Among the 16 malignant nodules, 4 (25%) appeared black/white, and 12 (75%) appeared orange/red on color maps. Of the 43 benign nodules, 16 (37.2%) were black/white, and 27 (62.8%) were orange/red. There was no statistically significant difference between the two groups in this regard ($P = 0.378$) (Table 2).

Histopathological examinations revealed that 8 (50%) of the malignant nodules were primary lung tumors, including 7 adenocarcinomas and 1 squamous cell carcinoma, while the remaining 8 (50%) were metastatic lesions, with 2 originating from breast cancer and 6 from colon cancer.

Among the benign nodules, 27 showed no change in size during follow-up. Of the 16 lesions with benign histopathological results, 8 were infectious lesions, 4 were hamartomas, 1 was a tuberculoma, 1 was a granuloma, 1 was a hydatid cyst, and 1 was a bronchogenic cyst.

5. Discussion

Pulmonary nodules are common lesions in clinical practice that require detailed radiological and clinical evaluation, as a malignant process may sometimes be an underlying cause. Accurate identification of these lesions is crucial to prevent unnecessary invasive or surgical procedures and to avoid iatrogenic complications, particularly in benign pulmonary nodules. Various conventional CT techniques have been used to differentiate benign from malignant pulmonary lesions. Currently, new CT techniques, including DECT, have been adapted to enhance lesion evaluation by measuring contrast uptake and enhancement (9).

In this study, we aimed to differentiate malignant lung nodules from benign ones using the dual CT technique, applying three different parameters, including both quantitative and visual analyses, such as iodine load and contrast load. Accurately measuring the density of each component in a lung lesion on conventional thoracic CT is challenging when multiple tissue types are present. This difficulty arises because the HU value in a tomographic voxel reflects both the iodine concentration and the average densities of the different underlying tissues.

Therefore, depending on mass density, the obtained values can be used to measure the densities of two different substances (such as iodine and bone) at an average energy level (4). The DECT technique allows for the acquisition of an additional attenuation value, which generates a difference between the two energies (10). The twin-beam dual-energy (TBDE) technique, on the other hand, enables high-contrast dynamic studies

Table 2. Histopathological Characteristics of Nodules [a]

Characteristic (N = 59)	Malignant nodules (N = 16)	Benign nodules [b] (N = 43)
Histopathological findings	16	-
Primary lung tumors [total: 8 (50%)]		
Adenocarcinomas	7	-
Squamous cell carcinoma	1	-
Metastatic lesions [total: 8 (50%)]		
Breast cancer	2	-
Colon cancer	6	-
Total benign lesions		43 [b]
Infectious lesions	-	8 (50)
Hamartomas	-	4 (25)
Tuberculoma	-	1 (6.25)
Granuloma	-	1 (6.25)
Hydatid cyst	-	1 (6.25)
Bronchogenic cyst	-	1 (6.25)
Contrast load (HU)		
Median (IQR); HU [c]	63 (154)	0.0 (64)
Iodine load (mg/mL)		
Median (IQR); mg/dL [d]	4.5 (11.8)	0.0 (4.5)
Color map findings [e]		
Black	4 (25)	27 (62.8)
Orange/red	12 (75)	16 (37.2)

Abbreviation: HU, hounsfield units.

[a] Values are expressed as No. (%) unless otherwise indicated.

[b] 27 pulmonary nodules without histopathology showed no change in size during follow-up.

[c] $P = 0.003$.

[d] $P < 0.001$.

[e] $P = 0.378$.

by filtering the X-ray beam before it reaches the patient. This approach allows for the simultaneous acquisition of high- and low-kV data in a single spectral CT scanning procedure. We used this technique in our study to distinguish between the benign and malignant potentials of lung nodules. While previous studies have explored the use of DECT for diagnosing pulmonary embolism, edema in bone structures, or accumulations in joints, limited research has focused on the characterization of solitary pulmonary lesions or nodules.

The first parameter we evaluated in this study was the contrast load, which required quantitative assessment. According to the ROC analysis performed to quantify the contrast load in lung lesions, the cut-off density value of 22 HU was found to have sensitivity and specificity rates of 100% and 58.14%, respectively. The distribution of the contrast agent differs between malignant tumors and normal lung tissue. To supply nutrients to the tissues, bronchial arteries grow, become tortuous, and ectatic. Furthermore, the clearance of the contrast agent from malignant tumors is limited. Once distributed, the contrast agent cannot be fully cleared from the tissues because it has also traversed into the extracellular space. This condition has been demonstrated in multiple studies on dynamic contrast-enhanced CT, showing that the contrast agent is not quickly washed out from malignant nodules (11). Similarly, we observed false-positive results in some nodular lesions of infectious, inflammatory, pulmonary sequestration, or vascular origin (such as arteriovenous malformations) due to the rapid accumulation of contrast in dynamic CT, likely caused by extensive vascular content.

The second parameter we investigated in our study was the quantification of iodine in the lesion. Based on measurements in the ROI of a nodular lung lesion, a cut-off value of 1 mg/mL iodine was found to differentiate between benign and malignant lesions with 100% sensitivity and 62.79% specificity. In this study, the most

appropriate threshold level was determined to be 1 mg/mL to confirm the presence of contrast enhancement with an iodine contrast agent. To date, no standardized iodine concentration thresholds have been established to determine the presence of contrast or contrast enhancement in a lung nodule. A previous study attempted to establish a calibration factor correlating the CT attenuation value (measured in HU) of a pulmonary nodule with the CT x-ray attenuation value (measured in mg/mL) and the iodine contrast agent concentration (measured in mg/mL). This study reported that values of 23.55 HU and 0.6 mg/mL would be ideal (12). In our study, we found a cut-off value of 22 HU for contrast load and 1 mg/mL for iodine load. Although these values are similar to those reported in the literature, our study showed a higher iodine quantity and a higher sensitivity compared to previous reports.

The third parameter we investigated was the qualitative analysis of color map changes in the image, corresponding to increasing iodine levels in the lesion. With the advent of dual-energy CT, the visual assessment of iodine overlay color maps has made it possible to obtain additional information based solely on the presence of iodine. This includes determining iodine concentrations and performing an attenuation analysis on a nodule.

According to the results of this study, it remains unclear whether the next diagnostic step in the management strategy for nodules larger than 10 mm should be a biopsy or PET-CT imaging. Because DECT can detect contrast enhancement in pulmonary nodules through both qualitative and quantitative methods, its results have been observed to be in parallel with those of PET-CT in determining contrast enhancement and differentiating malignant from benign lesions. Therefore, DECT may serve as an alternative option to PET-CT in lesion characterization, and further comparative studies are needed to support this hypothesis and confirm lesion nature. Additionally, the twin-beam technique used in obtaining the DECT scans in this study is particularly notable, as it results in lower radiation exposure compared to other DECT techniques and dynamic contrast-enhanced imaging methods.

Furthermore, another significant aspect of this study is the potential application of DECT as a method for evaluating the treatment response of metastatic lung nodules. In this study, we demonstrated the simultaneous presence of active and necrotic nodules in the lungs of a patient with a primary colorectal tumor and widespread lung metastases. Pulmonary nodules were detected on contrast-enhanced DECT performed for post-chemotherapy treatment response assessment. A significant and apparent iodine load was observed in the active metastatic nodule, whereas the iodine quantity in the necrotic nodule was undetectable. Although this finding was based on a single case, it suggests that DECT may serve as an alternative follow-up imaging method, potentially replacing PET-CT in certain clinical scenarios.

This study has some limitations that should be considered. Firstly, histopathological confirmation was not available for most benign nodules. Secondly, the quantitative distribution of iodine load and contrast load may have been heterogeneous due to the relatively small number of patients included in the study. While planning the study, we assumed that the incidence of malignancy would increase in parallel with increases in iodine and contrast load. However, because nodules smaller than 6 mm were excluded, results for smaller nodules could not be obtained. Although we excluded completely calcified nodules, partially calcified nodules may have increased the false-positive rate in iodine and contrast calculations. Another limitation was the lack of correlation established between nodule morphology and the three parameters analyzed in this study.

In the future, DECT may be crucial for assessing malignancy risk by providing a more detailed evaluation of lesion structure, aiding in the differentiation of cystic and solid nodules. Additionally, integrating artificial intelligence and machine learning for analyzing DECT data may allow for automatic classification and characterization of lesions. These advancements could significantly enhance the early diagnosis and management of lung lesions. However, further research and validation are necessary for incorporating these technologies into clinical practice.

In conclusion, diagnosing pulmonary nodules remains a challenge in clinical practice due to their high prevalence in the general population. Non-invasive imaging procedures are essential for identifying malignant nodules, as lung biopsies can sometimes lead to severe complications. Evaluating visual color maps and quantitatively calculating both iodine and contrast load using the DECT technique proved useful for differentiating malignant and benign pulmonary nodules. We believe that further studies with larger sample sizes are necessary to confirm the effectiveness of DECT in distinguishing between malignant and benign pulmonary nodules, as well as in identifying other solitary parenchymal lung nodules. Additionally, multicenter randomized controlled studies comparing PET-CT, MRI, or dynamic CT with new-generation DECT devices supported by artificial intelligence will

contribute to the improved diagnosis and imaging of lung nodules.

Footnotes

Authors' Contribution: Data collection, writing: S. T. and editing: M. O. of the article were done.

Conflict of Interests Statement: Author declare that has no conflict of interest.

Data Availability: The dataset presented in the study is available on request from the corresponding author during submission or after publication.

Ethical Approval: The study was started after the ethical approval of the research was given by the ethics committee of Van Yüzünvü Yıl University on 18.07.2018.

Funding/Support: No financial support was received for this study.

Informed Consent: Informed consent forms were obtained from the patients.

References

1. Gould MK, Tang T, Liu IL, Lee J, Zheng C, Danforth KN, et al. Recent Trends in the Identification of Incidental Pulmonary Nodules. *Am J Respir Crit Care Med*. 2015;**192**(10):1208-14. [PubMed ID: 26214244]. https://doi.org/10.1164/rccm.201505-0990OC.
2. Tang K, Wang L, Lin J, Zheng X, Wu Y. The value of 18F-FDG PET/CT in the diagnosis of different size of solitary pulmonary nodules. *Medicine (Baltimore)*. 2019;**98**(11). e14813. [PubMed ID: 30882661]. [PubMed Central ID: PMC6426628]. https://doi.org/10.1097/MD.0000000000014813.
3. Gould MK, Donington J, Lynch WR, Mazzone PJ, Midthun DE, Naidich DP, et al. Evaluation of individuals with pulmonary nodules: when is it lung cancer? Diagnosis and management of lung cancer, 3rd ed: American College of Chest Physicians evidence-based clinical practice guidelines. *Chest*. 2013;**143**(5 Suppl):e93S-e120S. [PubMed ID: 23649456]. [PubMed Central ID: PMC3749714]. https://doi.org/10.1378/chest.12-2351.
4. McCollough CH, Leng S, Yu L, Fletcher JG. Dual- and Multi-Energy CT: Principles, Technical Approaches, and Clinical Applications. *Radiology*. 2015;**276**(3):637-53. [PubMed ID: 26302388]. [PubMed Central ID: PMC4557396]. https://doi.org/10.1148/radiol.2015142631.
5. Dell'Aversana S, Ascione R, De Giorgi M, De Lucia DR, Cuocolo R, Boccalatte M, et al. Dual-Energy CT of the Heart: A Review. *J Imaging*. 2022;**8**(9). [PubMed ID: 36135402]. [PubMed Central ID: PMC9503750]. https://doi.org/10.3390/jimaging8090236.
6. Tsurusaki M, Sofue K, Hori M, Sasaki K, Ishii K, Murakami T, et al. Dual-Energy Computed Tomography of the Liver: Uses in Clinical Practices and Applications. *Diagnostics (Basel)*. 2021;**11**(2). [PubMed ID: 33499201]. [PubMed Central ID: PMC7912647]. https://doi.org/10.3390/diagnostics11020161.
7. Kaemmerer N, Brand M, Hammon M, May M, Wuest W, Krauss B, et al. Dual-Energy Computed Tomography Angiography of the Head and Neck With Single-Source Computed Tomography: A New Technical (Split Filter) Approach for Bone Removal. *Invest Radiol*. 2016;**51**(10):618-23. [PubMed ID: 27187046]. https://doi.org/10.1097/RLI.0000000000000290.
8. Lee MH, Park HJ, Kim JN, Kim MS, Hong SW, Park JH, et al. Virtual non-contrast images from dual-energy CT angiography of the abdominal aorta and femoral arteries: comparison with true non-contrast CT images. *Br J Radiol*. 2022;**95**(1138):20220378. [PubMed ID: 36039820]. [PubMed Central ID: PMC9815733]. https://doi.org/10.1259/bjr.20220378.
9. Qiu L, Pu XH, Xu H, Yu TF, Yuan M. Dual-energy computed tomography iodine uptake in differential diagnosis of inflammatory and malignant pulmonary nodules. *Diagn Interv Radiol*. 2022;**28**(6):563-8. [PubMed ID: 36550756]. [PubMed Central ID: PMC9885669]. https://doi.org/10.5152/dir.2022.201091.
10. Alizadeh LS, Vogl TJ, Waldeck SS, Overhoff D, D'Angelo T, Martin SS, et al. Dual-Energy CT in Cardiothoracic Imaging: Current Developments. *Diagnostics (Basel)*. 2023;**13**(12). [PubMed ID: 37371011]. [PubMed Central ID: PMC10297493]. https://doi.org/10.3390/diagnostics13122116.
11. Gilbert FJ, Harris S, Miles KA, Weir-McCall JR, Qureshi NR, Rintoul RC, et al. Dynamic contrast-enhanced CT compared with positron emission tomography CT to characterise solitary pulmonary nodules: the SPUtNIk diagnostic accuracy study and economic modelling. *Health Technol Assess*. 2022;**26**(17):1-180. [PubMed ID: 35289267]. https://doi.org/10.3310/WCEI8321.
12. Reiter MJ, Winkler WT, Kagy KE, Schwope RB, Lisanti CJ. Dual-energy Computed Tomography for the Evaluation of Enhancement of Pulmonary Nodules=3 cm in Size. *J Thorac Imaging*. 2017;**32**(3):189-97. [PubMed ID: 28338536]. https://doi.org/10.1097/RTI.0000000000000263.